EPJ Web of Conferences **157**, 03039 (2017) DOI: 10.1051/epjconf/201715703039
22 Topical Conference on Radio-Frequency Power in Plasmas

ICRF-Induced Changes in Floating Potential and Ion Saturation Current in the EAST Divertor

Rory Perkins[1,⋆], *Joel* Hosea[1], *Gary* Taylor[1], *Nicola* Bertelli[1], *Gerrit* Kramer[1], *Chengming* Qin[2], *Liang* Wang[2], *Jichan* Yang[2], and *Xinjun* Zhang[2]

[1] *Princeton Plasma Physics Laboratory, Princeton, New Jersey, U.S.A*
[2] *Institute for Plasma Physics, Chinese Academy of Science, Hefei, China*

Abstract. Injection of waves in the ion cyclotron range of frequencies (ICRF) into a tokamak can potentially raise the plasma potential via RF rectification. Probes are affected both by changes in plasma potential and also by RF-averaging of the probe characteristic, with the latter tending to drop the floating potential. We present the effect of ICRF heating on divertor Langmuir probes in the EAST experiment. Over a scan of the outer gap, probes connected to the antennas have increases in floating potential with ICRF, but probes in between the outer-vessel strike point and flux surface tangent to the antenna have decreased floating potential. This behaviour is investigated using field-line mapping. Preliminary results show that mdiplane gas puffing can suppress the strong influence of ICRF on the probes' floating potential.

1 Introduction

RF rectification is a sheath phenomenon that is important for impurity production via ion bombardment, hot-spot formation on antennas, modifications to the scrape-off layer (SOL), and dissipation of wave power (far-field sheaths). Many aspects of RF rectification focus on the possible increase in plasma potential resulting from relatively strong RF fields driving electrons into plasma-facing components. However, in the divertor of NSTX, the floating potential of certain swept probes decreases and the currents to certain tiles increases with the application of ICRF heating. This is as expected for relatively weaker RF fields for which the oscillating plasma potential drives a net (RF-averaged) electron current without depleting the linking flux tube of electrons or modifying the I-V characteristic observed in the absence of RF fields [1]. The averaged electron current induced by this form of RF rectification can heat the tiles locally and is the leading hypothesis for the heat flux observed in the spirals found in the divertors of NSTX during fast-wave heating [2]. This effect is observed for probes attached to field lines that pass through the SOL in front of the fast-wave antenna but are not linking the antenna. On the Alcator C-Mod device, when the field lines intercept the antenna, the RF rectification in the large electric field there does result in large positive increases in the plasma potential, presumably to reduce the electron current at the antenna [3].

The Experimental Advanced Superconducting Tokamak (EAST) provides an excellent opportunity to study RF rectification in the SOL in finer detail. EAST is designed for high-power long-pulse discharges, and a major component is an ICRF system consisting of two antennas and 12 MW of source power [4]. One antenna is located at I port and consists of four toroidally-spaced folded straps. The second antenna is at B port and consists for a two-by-two array. The nominal parallel wavenumber for the I port array is around 14 m^{-1} for dipole phasing while for B-port $k_{||} \approx 12$ m^{-1}. Current levels of coupled ICRF power are sufficient to modify both the SOL and the core plasma. EAST has extensive arrays of triple probes in both the carbon lower divertor [5] and the tungsten upper divertor [6]. The upper divertor has two arrays spaced apart by 112 degrees. The probes do not have RF compensation and are thus sensitive to RF rectification. While RF rectification is commonly studied in the vicinity of the antenna where the RF fields are expected to be strongest, far-field effects are imporant not only for NSTX but perhaps also for Alcator C-Mod, where far-field sheaths on limiters or divertor tiles may also be contributing to impurity production [7].

This paper explores several different cases of RF rectifcation in the divertor. Section 2 continues studies of an previously observed effect where probes on flux surfaces that intercept the antenna have a positive increase in floating potential whereas those more inboard swing negative. Magnetic mapping of the probe location to the midplane helps assess the location of these probes relative to the antennas, the density profile measured by a reflectometer, and between upper- and lower-divertor probes. Second, in Sec. 3 we present preliminary findings regarding the effects of gas puffing at one of the antennas on the response of probes. Both the floating potential (V_{fl}) and ion saturation current (I_{sat}) can be dramatically changed. Interestingly, in some instances, the large modulation of floating potential with RF is greatly reduced.

⋆e-mail: rperkins@pppl.gov

2 The dependence of floating potential polarity with ICRF on magnetic connection in the SOL

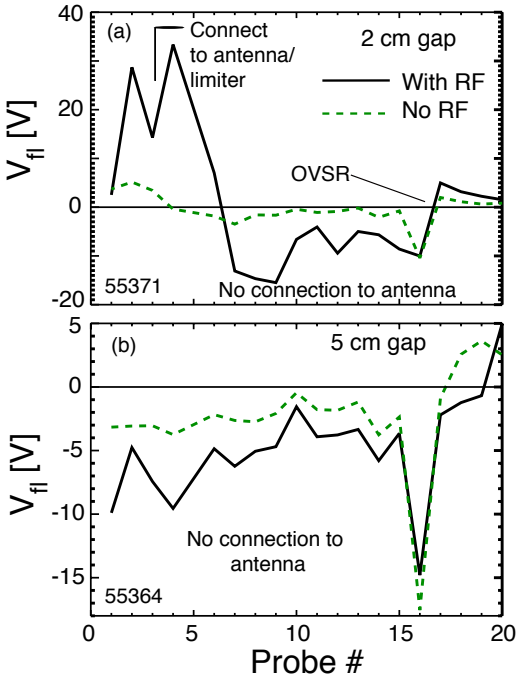

Figure 1: Profiles of floating potential for the lower-divertor array for two different outer-gap values. Black curves are profiles taken at t = 3.525 s, during the RF pulse and averaged over 40 ms. Green curves are taken at t = 3.190 s, before the RF pulse. OVSR indicates the outer-vessel strike radius.

Over a scan of the outer gap size, the lower-divertor probes tended to show a decrease in floating potential with ICRF unless the probe was further outboard than the flux surface tangent to the antenna, in which case the change in floating potential is positive [8] . These shots were lower-single null discharges. During shot 55364, 0.75 MW of ICRF power were coupled through both antennas; during shot 55371, the I-port antenna coupled 0.85 MW while the B-port antenna coupled 1.15 MW. In each case, the ICRF power was applied from 3.277 s to 4.248 s. With a nominal outer gap size of 2 cm (Fig. 1(a)), the probes outboard of the flux surface tangent to the antenna tended to rise in floating potential with ICRF whereas those inboard tended to fall in floating potental. The most inboard probes (probes numbered 17-20 in this plot) have a positive change in floating potential, but they also lie inboard of the outer-vessel strike radius (OVSR). At a 5 cm gap (Fig. 1(b)), the lower array shows a negative value for floating potential during ICRF, and for this outer-gap value none of the probes connect to the antenna. As an aside, the very negative floating potential for probe 16, present even without ICRF, may be due to the probe's location relative to the outer strike point [9].

These discharges are now analyzed using field-line mapping in Fig. 2, which maps both upper (D-port) and lower probes to the midplane. Also shown are the midplane major radii of the ICRF limiter faces for each antenna. The general trends found before are more or less reproduced and can be directly compared between upper and lower divertor probes. In the case of shot 55364 (Fig. 2a), all probes lie inboard of the antenna, and their floating potential are below zero or marginally above it. Strong positive floating potentials are only found for those probes with mapped midplane radii beyond the antenna limiters indicated in the figures (Fig. 2b).

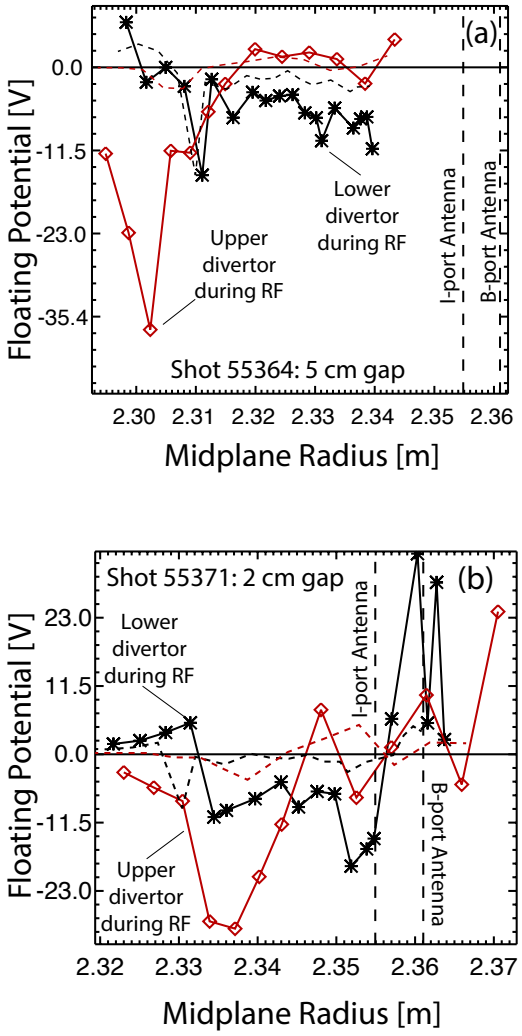

Figure 2: Floating potential for both the lower-divertor array (black) and the Bay-D upper-divertor array (red) as a function of major radius mapped to the midplane. Dashed lines show pre-ICRF profiles at t = 3.19 s averaged over 16 ms. (a) Shot 55364, 5 cm outer gap, and (b) shot 55371, 2 cm outer gap.

Figure 3 shows the magnetic mapping for both sets of probes, plotting the probe major radius at the divertor against the major radius mapped to the midplane. This plotting scheme is chosen so that density profiles from the J-port edge reflectometer can be overlaid as a function of midplane radius. The midplane density is quite low compared to the righthand cutoff density for fast waves. For instance, taking an ICRF frequency of 27 MHz and launched

$k_{||}$ = 12.2 m, an on-axis toroidal field of 2 T (extrapolating to 1.6 T at the antenna location) gives a cutoff density of roughly 10^{19} m^{-3}, which greatly exceeds the measured density at the midplane anywhere in the SOL and places the cutoff layer well inside the separatrix according to Fig. 3. The relationship between this large evanescent layer for fast waves and the divertor probe signals will be the topic of future work.

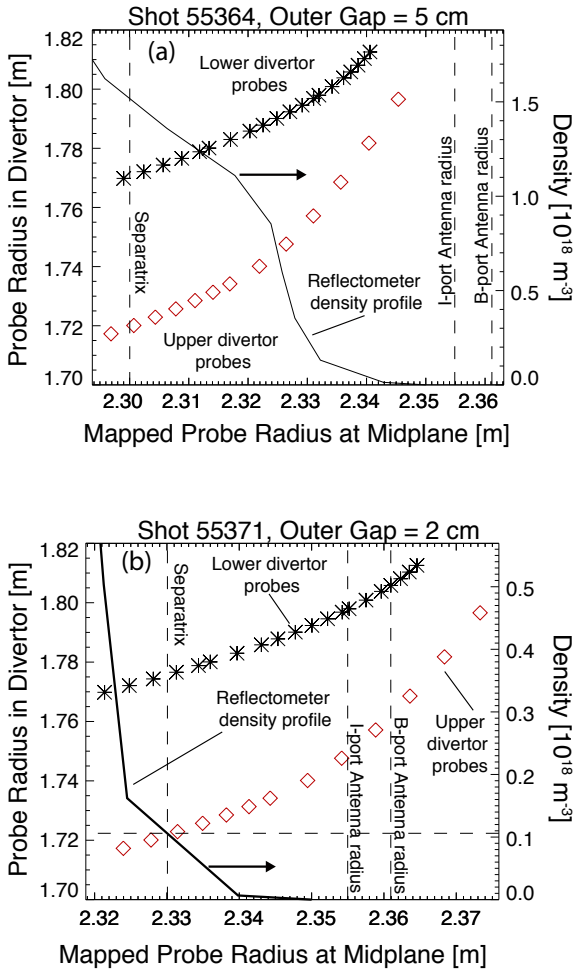

Figure 3: Magnetic mapping of the divertor probes to the midplane for comparison with the midplane density profile obtained by reflectometry. (a) Shot 55364 and (b) Shot 55371, both at t = 3.525 s during the ICRF pulse.

3 The effect of gas puffing on divertor probes

This section shows preliminary results for a series of shots with increasing gas puffing in single upper null discharges driven by 1.4 MW of 4.6 GHz lower hybrid heating. The ICRF power is applied to each antenna separately; in all cases presented here, the I-port antenna is powered on first at t = 3.2s until t = 5.12s, while B-port is powered from t = 5.77 s to t = 7.2 s, with each modulated between full power (1 MW) and half power. The gas injector, located near the B-port antenna, is active from t = 2.5 s to 9 s, and increases from shot 69938 to 69939 and again to 69940. Further increase in gas puffing resulted in a prompt disruption. Shot 69942 is a fiducial shot without gas puffing. Note that the B-port antenna arced off around t = 6.8 s for shot 69940. Also, changes in the outer gap, shown in Figure 4, must be taken into account. The outer gap is held rather constant during the modulation, varying 3 mm peak-to-peak. Shots 69938 and 69939 have a 0.5 cm increase in outer gap over the fiducial. The gap for shot 69940 increased steadily during the I-port pulse and dramatically during the B-port pulse.

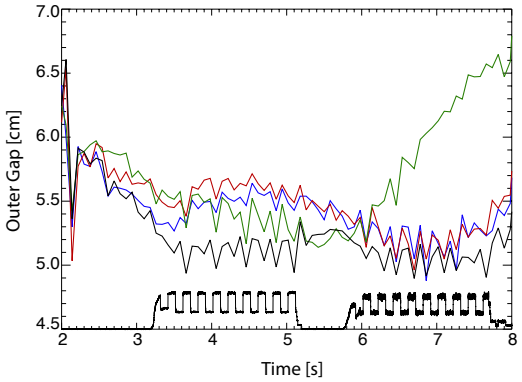

Figure 4: Outer gap values for no-gas-puff (black), smallest puff (blue), medium puff (red) and largest puff (green).

The most dramatic effect of the gas puffing on the divertor probes can be seen on Probe 6, Fig. 5a. Without gas puffing, this probe shows a strong negative response to both the I-port pulse and the second half of the B-port pulse. With gas puffing, this response is strongly suppressed at intermediate gas puffs. Similar behavior is seen on neighboring probes. For Probe 12 (Fig. 5b), though, the modulations in V_{fl} become bigger with gas puffing.

The I_{sat} signals response to ICRF is also modified by the gas puffing; Fig. 6 shows I_{sat} for probe 4 and Fig. 7 shows I_{sat} for Probe 5 in the lower divertor. Probe 4 is strongly positively correlated with the first half of the B-port pulse for 69938 and 69939, whereas Probe 5 is anti-correlated.

4 Discussion and Conclusions

Changes to divertor probe signals due to ICRF can be due to wave fields directly interacting with the sheaths, modifications to the SOL, and core heating. Part of this work is to determine the former in relationship to the other components for comparison with the NSTX results. Negative changes in floating potential are likely due to RF rectification. It is commonly reasoned that plasma potential rises with RF, so in principle the floating potential should also rise, being given by first-principle considerations as: $V_{fl} = V_{pl} - \alpha T_e$ for some α depending on geometry and gas species. However, in an RF field, the floating potential can drop when RF currents flow through the sheath and deliver a net electron current to the probe as per Ref. [1]. From

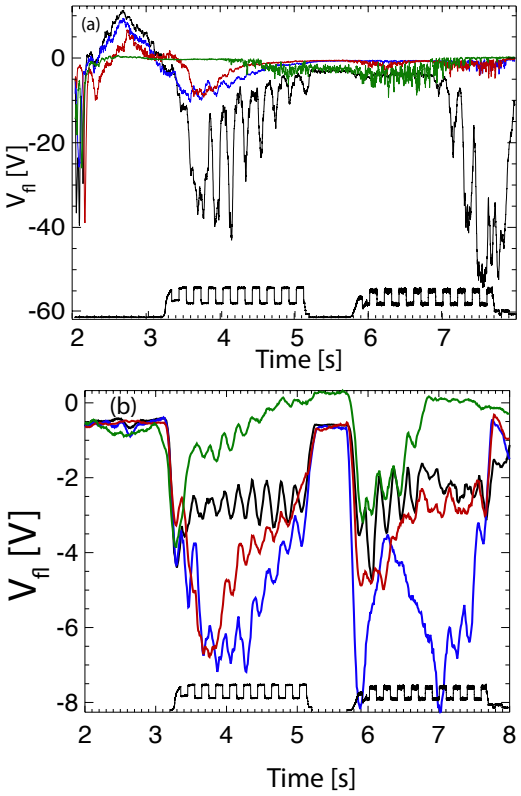

Figure 5: V_{fl} for Probes 6 (a) and 12 (b) in the upper divertor. Black: shot 69942, blue: 69938, red: 69939, green: 69940.

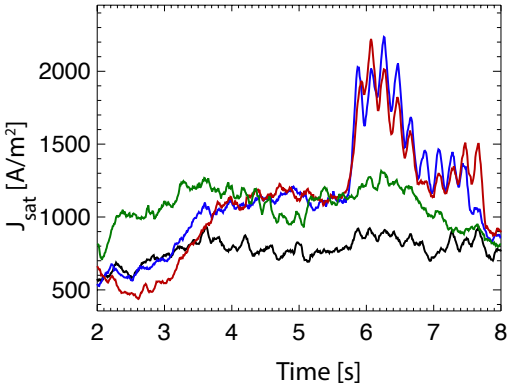

Figure 6: I_{sat} for Probe 4 of the lower divertor during a gas-puff scan. Black: shot 69942, blue: 69938, red: 69939, green: 69940.

our observations, probes connected to the antenna see an increase in plasma potential in response to rectification at the antenna which then propagates along field lines. Inboard probes with prompt anti-correlated responses to RF, however, are likely subject to ICRF wave fields.

In conclusion, magnetic mapping of the EAST divertor probes back to the midplane allows comparison between upper and lower probe sets and also to diagnostics such as the edge reflectometer. A strong rise in floating potential is seen only for outboard probes in the case of a 2 cm outer gap when such probes lie outboard of the flux surface tangent to the antenna face. Gas puffing is seen to strongly modify the probe signals and in some instances substantially reduces their modulation with ICRF; this effect will be studied further in the future.

This research is partly supported by the National Key Research and Development Program No. 2016YFA0400601 and also by the China Magnetic Confinement Fusion Science Program No. 2015GB101001. This research is also supported by US DOE Contract No. DE-AC02-09CH11466.

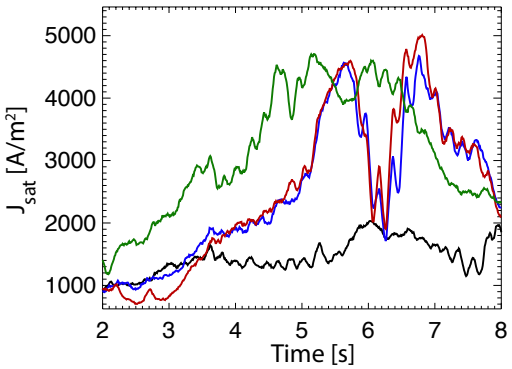

Figure 7: I_{sat} for Probe 5 of the lower divertor during a gas-puff scan. Black: shot 69942, blue: 69938, red: 69939, green: 69940.

References

[1] A. Boschi, F. Magistrelli, Il Nuovo Cimento **29**, 487 (1963)
[2] R. J. Perkins et al., Phys. Plasmas **22** (2015)
[3] R. Ochoukov et al., Plasma Physics and Controlled Fusion **56**, 015004 (2014)
[4] Y. Zhao et al., Fusion Engineering and Design **89**, 2642 (2014)
[5] T. Ming et al., Fusion Engineering and Design **84** (2009)
[6] J.C. Xu et al., Rev. Sci. Instrum. **87** (2016)
[7] S. Wukitch et al., Bull. APS **61** (2016)
[8] J. Hosea et al., Bull. APS **61** (2016)
[9] J.C. Hosea et al., AIP Conference Proceedings **1580**, 105 (2014)